

Collision-induced dissociation of lanthanide oxide ions in quadrupole ion traps: effects of bond strength and mass

Glen P. Jackson^a, Fred L. King^a, Douglas E. Goeringer^b, Douglas C. Duckworth^{b,*}

^a Department of Chemistry, West Virginia University, Morgantown, WV 26506-6045, USA

^b Chemical Sciences Division, P.O. Box 2008, Oak Ridge National Laboratory, Oak Ridge, TN 37831-6375, USA

Received 15 July 2001; accepted 22 January 2002

Abstract

Collision-induced dissociation (CID) rates are measured for a suite of lanthanide (plus yttrium) monoxide ions stored in a quadrupole ion trap. Yttrium, neodymium, and gadolinium oxides, having the same nominal dissociation energy ($D_0 \approx 735 \text{ kJ mol}^{-1}$) but different masses, provide an empirical correction of $-1.2 \text{ s}^{-1} \text{ amu}^{-1}$ for the measured CID rates. The CID rate correction enables the correlation of bond dissociation energy with CID rate, allowing quantitative determinations of bond dissociation energies for lanthanide metal monoxide ions. For bond dissociation energies in the range of $567\text{--}849 \text{ kJ mol}^{-1}$, mass corrected rates range from 50 to 120 s^{-1} . The calibration sensitivity is equivalent to $5 \text{ kJ mol}^{-1} \text{ s}^{-1}$, and the measurement precision is $\sim 25 \text{ kJ mol}^{-1}$. Bond energy determinations are found to agree with the average values reported for lanthanide oxide ions. (Int J Mass Spectrom 216 (2002) 85–93) © 2002 Elsevier Science B.V. All rights reserved.

Keywords: Collision-induced dissociation; Lanthanide oxide ions; Bond strength

1. Introduction

Recent studies in our laboratory have focused on the measurement of collision-induced dissociation (CID) rates of strongly bound metal oxide ions such as TaO^+ ($D_0 = 790 \text{ kJ mol}^{-1}$) stored in quadrupole ion traps (QITs) [1]. The purpose of this work is to provide an experimental basis for extending the understanding and use of a thermal reaction model [2–5] of CID in ion trap mass spectrometers to diatomic ions. A potential benefit is the capability of determining relative and absolute dissociation energies via CID measurements in QIT instruments. Furthermore, the complete dissociation of metal oxide ions is useful in elemental determinations where isobaric spectral interferences

occur [6–9]. The use of CID in ion traps could serve as an alternative and universal approach to overcoming chemical interferences.

There currently exist several methods for determining dissociation energies using CID in quadrupole ion traps. Hart and McLuckey [10] found a logarithmic dependence of the critical energy for decomposition on the threshold excitation voltage amplitude. The threshold excitation voltage is defined as the minimum voltage required to dissociate a polyatomic ion. Extrapolating a plot of dissociation rate vs. excitation amplitude to zero rate yields the threshold excitation voltage. Using polyatomic ions of low dissociation energy ($<300 \text{ kJ mol}^{-1}$), a calibration curve was obtained for use in the determination of an ‘unknown’ dissociation energy. Shifts in the resonance absorption frequency complicate these experiments, especially at

* Corresponding author. E-mail: duckworthdc@ornl.gov

higher dissociation energies ($>200 \text{ kJ mol}^{-1}$) where higher-order fields come in to play with increasing excitation time and amplitude. Additionally, space charge effects cause the fundamental secular frequency of an ion cloud to shift as a function of ion density [11]. These factors make it very difficult (impossible using some software packages) to maintain on-resonance conditions during an experiment.

Colorado and Brodbelt proposed an alternative method for measuring bond dissociation energies [12]. In their approach, an on-resonance, low-amplitude excitation voltage is applied to the endcaps for a fixed time. The degree of fragmentation is then measured. The excitation voltage is increased, incrementally, until a significant degree ($>50\%$) of fragmentation occurs. The threshold excitation voltage in this case is defined as the excitation amplitude required to yield 10% dissociation of the molecular ion. In this case, a plot of the threshold excitation voltage vs. threshold fragmentation energies gives a linear dependence, instead of the logarithmic dependence observed by Hart and McLuckey. Separate calibration curves are required when observing different systems (e.g., hydrogen-bonded complexes vs. covalently bound molecules), although the reasons are not completely clear at this time. The experiments conducted by Hart and McLuckey, and Colorado and Brodbelt were optimized for polyatomic (organic) molecules having threshold energies for fragmentation $\leq 300 \text{ kJ mol}^{-1}$. The metal oxides of interest in this study, however, have dissociation energies on the order of $550\text{--}850 \text{ kJ mol}^{-1}$. Under the conditions used by the above authors, the oxide ions in this study would be scattered from the trap long before reaching the required voltage for dissociation. The low-trapping potential ($q_z < 0.4$) and the modest center-of-mass collision energy associated with a helium bath gas do not impart enough energy into the ions to cause dissociation. Therefore, special conditions are required to achieve dissociation of these strongly bound diatomic species.

Duckworth et al. showed that by using a q_z of 0.67 and $\sim 0.5 \text{ mTorr}$ neon ($1 \text{ Torr} = 133.3 \text{ Pa}$) as

the bath gas, dissociation yields close to 100% could be obtained for TaO^+ within 20–50 ms of excitation [1]. The large potential well depth associated with such a q_z value allows higher amplitude excitation voltages to be applied [13] and greater kinetic energies to be imparted to the ions. The neon collision target more efficiently converts the kinetic energy to internal energy than helium [14]. Goeringer et al. simulated the ion trap CID kinetics of TaO^+ by applying a thermal unimolecular reaction model [5]. An internal temperature for TaO^+ on the order of 15,000 K was predicted for the conditions used.

For measured dissociation rates to be useful in the determination of dissociation energies, it is necessary to compare them without the complication of mass effects. This work provides new insight into making reliable CID rate measurements and presents a new approach to determining dissociation rates that ensures that on-resonance rate measurement conditions are established. Determination relative to an internal standard accounts for temporal fluctuations in CID response. An empirical correction for mass effects on CID rates is determined and applied to measured CID rates. Corrected dissociation rates are used to quantify bond dissociation energies of lanthanide monoxide ions.

2. Experimental

A pulsed direct current glow discharge (GD) ionization source was coupled to a Teledyne 3DQ quadrupole ion trap mass spectrometer, as described previously [4]. Metal oxides of interest were mixed in a $\sim 1:1$ ratio with praseodymium oxide (the internal standard) and pressed onto the surface of a gold or indium pin. Samples were sputtered in the neon discharge (0.8 Torr) until a steady state signal was observed. Metal and metal oxide ions were trapped and allowed to react with molecular oxygen that was admitted into the trap at a pressure of $8 \times 10^{-7} \text{ Torr}$. Neon made up the remaining bath gas pressure to a total of $5 \times 10^{-4} \text{ Torr}$.

A typical scan function involved the following:

1. 5 ms metal ion accumulation period, with a single frequency excitation signal applied to resonantly eject the matrix ions (m/z 197 for gold pins, m/z 115 for indium).
2. 50–100 ms reaction period during which metal ions were allowed to react with molecular oxygen at $q_z = 0.2$.
3. 5 ms oxide ion isolation period using mass selective instability [15] and filtered noise fields (FNFs) [16] to obtain the ion of interest.
4. 30 ms ion cooling period at $q_z = 0.2$.
5. 20 ms, 226 kHz, 250 mV_{pp} resonance excitation signal applied in a dipolar fashion at $q_z \sim 0.67$ [17]. The rf amplitude was scanned over the absorption range in order to determine the point of maximum dissociation. A second excitation frequency (~ 260 kHz) was simultaneously applied to eject the product metal ions as they formed thereby preventing the forward oxidation reaction.
6. 10 ms cooling period at $q_z = 0.2$ to collisionally cool the ions before mass analysis.
7. Mass analysis from m/z 130 to 200 at 12,000 amu s⁻¹ using axial modulation (mass spectra for yttrium oxide were taken from m/z 80 to 150).

Initial dissociation rate measurements obtained using the absorption curve method described above gave inconsistent results because no attempt was made to isolate a *single* isotope of a given oxide ion in step three above. It was found that, as has been noted in previous reports [11], that the ion number density in the trap greatly affects the degree of molecular ion fragmentation. In the case of lanthanides with several isotopes, the effects of space charge from the non-dissociated isotopes are significant. Considerable improvement in reproducibility was achieved by isolating an individual isotope prior to the dissociation step. However, space charge effects still existed because of differences in number densities of ions having the same nominal mass. It was found that the initial ion number density changed both the resonance frequency and the degree of fragmentation that occurred.

The degree of dissociation increased as the initial ion signal decreased because of the decreased coulombic repulsion occurring in the ion cloud at lower ion number densities. When higher number densities exist, a wider distribution of secular frequencies occurs and not all the ions will be in resonance at once. When fewer ions are stored there is less charge repulsion and a larger fraction of ions will be in resonance and will acquire the energy required to dissociate. A linear relationship was found between the maximum fractional dissociation and the initial ion number density. Therefore, a correction could be made to normalize the fractional dissociation if the initial ion abundance deviated significantly from a desired point. It was preferable, however, to maintain a consistent ion abundance prior to each dissociation experiment so that corrections were not necessary. This was achieved by using an enriched isotope as the sample in the glow discharge. Quantitative isolation was achieved using FNF frequencies to eject any remaining isotopes and product ions. The glow discharge voltage was adjusted to maintain the desired ion number density. Data averaging of 32 scans constituted a single analysis. In all cases, four repeat analyses were made intermittently between the internal standard and the ion of interest.

2.1. Method development

Previous experiments in this laboratory directly measured the dissociation rate of tantalum oxide ions by monitoring the metal oxide intensity as a function of increasing resonance excitation times [1,5]. For each rate determination the excitation frequency was set to 226 kHz and the rf trapping potential amplitude was tuned to produce maximum dissociation at a single resonance excitation time. Tuning the ion into resonance at 226 kHz by adjusting the rf trapping potential amplitude improves frequency resolution over tuning the resonance frequency (limited to a 1 kHz resolution on this system) at a fixed trapping potential. This also ensures that a constant q_z and an optimum resonance overlap is achieved.

In initial attempts to apply the same methodology used for TaO⁺ to lanthanide oxide ions, precision and

accuracy were degraded because of shifts in resonance excitation frequency. It has been shown that resonance frequency shifts result as a function of ion abundance, and resonance excitation time and voltage [10,11]. Therefore, for the most accurate rate measurements dynamic tuning of the resonance excitation is required as a function of resonance excitation time, voltage, and ion abundance. For example, the procedure described by Hart and McLuckey required the alteration of both the dissociation time and the tuning frequency during an automated scan function. As this programming ability is not present for our instrument (or for most commercially available instruments), an alternative method for measuring dissociation properties is used that does not require a change of more than one variable in a given scan function.

The use of resonance absorption curves is presented as an alternative to that proposed in references [1,10] because shifts in resonance frequency are easily observed and corrected. Although resonance absorption curves normally do not provide the detailed kinetic information contained in dissociation rate measurements it is possible to convert the fractional dissociation determined from a resonance absorption curve to a phenomenological rate. Assuming a pseudo-first-order dissociation rate, as established in references [1,10], the abundance of a lanthanide oxide $[\text{LnO}^+]_t$, at time t can be given as

$$[\text{LnO}^+]_t = [\text{LnO}^+]_0 \exp^{-[nk_{\text{tot}}t]} \quad (1)$$

where $[\text{LnO}^+]_0$ is the initial ion abundance, n the collision gas number density, and k_{tot} the rate constant for all LnO^+ losses. The sum of the loss rates, nk_{tot} , is given by

$$nk_{\text{tot}} = nk_{\text{diss}} + nk_{\text{scatt}} + nk_{\text{react}} \quad (2)$$

and if the scattering rate, nk_{scatt} , and alternative reaction rate, nk_{react} , can be shown to be negligible, nk_{tot} will approximate the dissociation rate nk_{diss} . This condition was established using conditions wherein $\sim 100\%$ of the product metal ions were recovered [1]. The fractional dissociation, determined from the absorption curve at a fixed dissociation time t , can be

converted to a dissociation rate according to the equation

$$nk_{\text{diss}} = \frac{-\ln([\text{LnO}^+]_t/[\text{LnO}^+]_0)}{t} \quad (3)$$

where nk_{diss} is the phenomenological rate for a given bath gas pressure and excitation amplitude. Measuring the rate at the point of maximum dissociation in the absorption curves alleviates the problems associated with resonance shifts. In addition, the dissociation measurement is not dependent on the arbitrary dissociation time used to collect the resonance absorption curve, but is dependent only on the excitation amplitude. This allows modest extension of the method as needed due to differences in rate due to mass and dissociation energy.

3. Results and discussion

The experimental approach employed in earlier work for TaO^+ was applied to the oxide ion of lanthanum ($D_0 = 860 \text{ kJ mol}^{-1}$) [1]. Fig. 1 shows the phenomenological dissociation rates for lanthanum and tantalum oxide ions as a function of resonance excitation amplitude. Interestingly, the lanthanum oxide ion was found to dissociate at much lower excitation voltages than the tantalum oxide ion ($D_0 = 790 \text{ kJ mol}^{-1}$). Thus, a series of CID experiments were performed on a suite of lanthanide (plus yttrium) monoxide ions to determine the role of bond dissociation energy and ion mass on measured dissociation rates.

3.1. Bond strength effects on dissociation rate

To characterize the relationship between bond dissociation energy and CID rate, oxide ions having similar masses (variation $\leq 5 \text{ amu}$) but a wide range of dissociation energies were examined. Fig. 2 shows the dissociation rate vs. bond strength for a number of oxide ions having very similar masses. The rates were calculated using Eq. (3) and were normalized to the dissociation rate of the internal standard, PrO^+ . Calculations using a thermal model for the dissociation

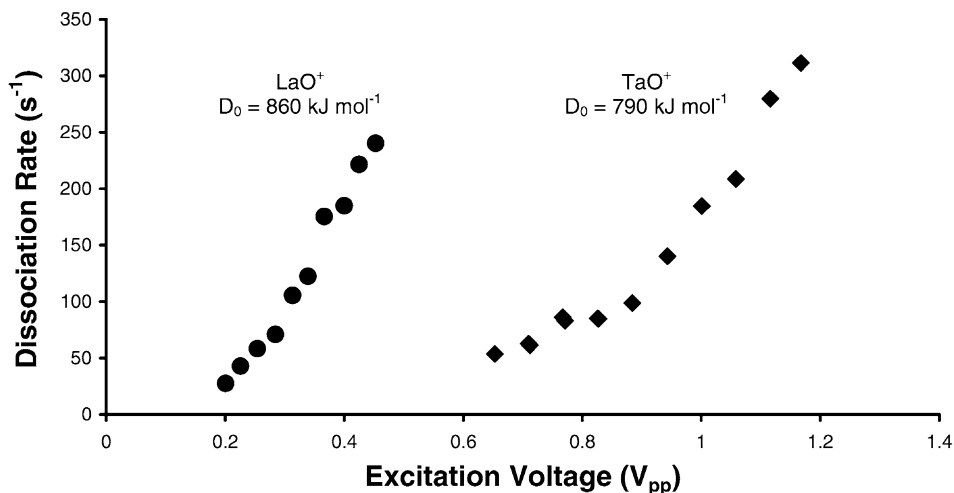


Fig. 1. Comparison of dissociation rates as a function of resonance excitation voltage for LaO^+ and TaO^+ . Secular frequency = 226 kHz (q_z 0.67), 0.5 mTorr Ne collision gas.

of diatomic ions having a Boltzmann distribution of internal energies suggest that CID rates decrease exponentially with dissociation energy [5,18]. Thus, an exponential fit ($R^2 = 0.90$) is used in Fig. 2.

The measured dependence of CID rate on dissociation energy is approximately $-0.2 \text{ mol kJ}^{-1} \text{ s}^{-1}$ (for mass 157); thus, indicating that the dissociation rate

decreases by 1 s^{-1} for every 5 kJ mol^{-1} increase in dissociation energy. The standard deviations of the dissociation rates obtained in this experiment average $\sim 5 \text{ s}^{-1}$ ($n = 4$), which is equivalent to a standard deviation of the bond energy measurement of $\sim 25 \text{ kJ mol}^{-1}$. This error is marginally larger than the internal error usually reported for thermodynamic data

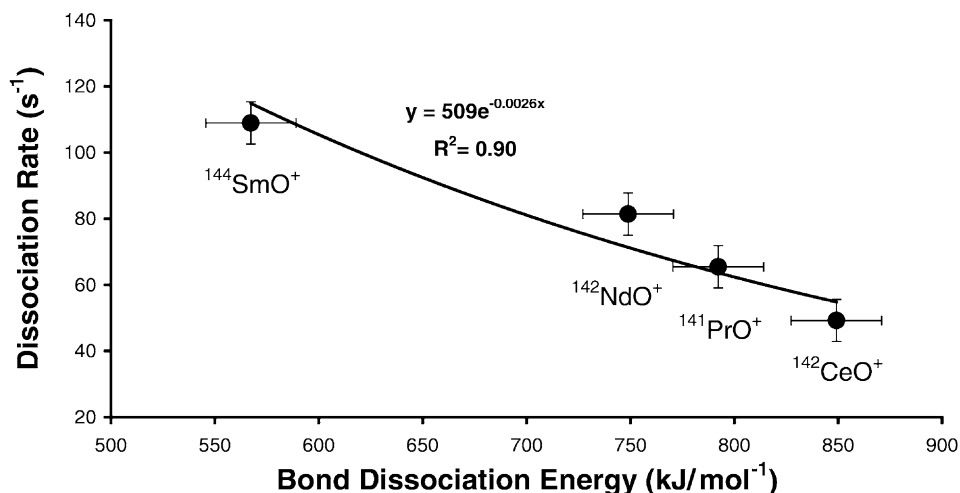


Fig. 2. Plot of the dissociation rates as a function of bond dissociation energy for oxide ions having the same nominal mass to determine the sensitivity of the measurement to dissociation energy.

Table 1
Dissociation energy and masses of the oxide ions used

| Element oxide ion | Oxide ion mass (amu) | D_0 (kJ mol ⁻¹) |
|-------------------|----------------------|-------------------------------|
| YO ⁺ | 105 | 725 (±18) ^{a,#} |
| CeO ⁺ | 158* | 849 (±22) ^b |
| PrO ⁺ | 157* | 792 (±22) ^b |
| NdO ⁺ | 158* | 749 (±22) ^{b,#} |
| NdO ⁺ | 162 | 749 (±22) ^{b,#} |
| SmO ⁺ | 160* | 567 (±22) ^b |
| GdO ⁺ | 170 | 735 (±22) ^{b,#} |

The symbol (*) is used to characterize the sensitivity to bond strength for near constant mass and (#) used to characterize the sensitivity to mass at near constant bond strength.

^a See [20,21].

^b See [19] and references therein.

of this kind [19,20]. As for accuracy, the values calculated here agree with the average of reported values ($\pm 1\sigma$).

3.2. Mass effects on dissociation rate

The effect of mass on the dissociation rates of metal monoxide ions can be determined by measuring the CID rates for each of the metal oxides of yttrium, neodymium, and gadolinium. These oxides have similar bond dissociation energies and are listed in Table 1 along with other metals considered in this

study. These elements (indicated with a '#' in Table 1) were selected on the basis of several characteristics: (1) the dissociation energies have been reasonably well established and lie within a 50 kJ mol⁻¹ range, (2) the monoxide ion can be formed via metal ion molecule reactions with molecular oxygen under the conditions of the experiment, (3) the monoxide ion can be isolated and stored at the designated starting number density, and (4) the monoxide can be dissociated without chemical reaction or scattering losses under the defined CID conditions.

The fractional dissociations of ⁸⁹YO⁺, ^{142,146}NdO⁺, and ¹⁵⁴GdO⁺ were normalized to the internal standard (PrO⁺), converted to a dissociation rate using Eq. (3), and plotted vs. monoxide ion mass in Fig. 3. Unfortunately, no monoxide ion could be found of similar bond strength and intermediate mass (105 < LnO⁺ < 158) thereby limiting the number of data points in this plot. The line of best fit ($R^2 = 0.995$) gives a mass correction of $-1.15 \text{ s}^{-1} \text{ amu}^{-1}$. Also, no other suite of metal monoxides could be found having different bond dissociation energy that also meets the above criteria and spanned such a wide mass range. Thus, this sensitivity of the dissociation rate to mass has only been established for a single bond dissociation energy of 735 kJ mol⁻¹. Evidence

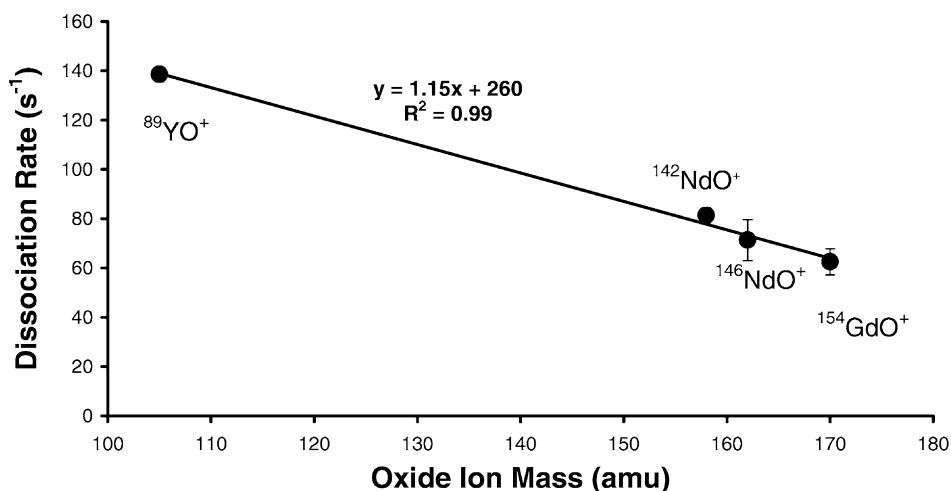


Fig. 3. Plot of the dissociation rate vs. oxide ion mass for compounds having the same nominal dissociation energy to determine the effect of mass on the dissociation rate.

will be provided later showing that the CID rate dependence on monoxide ion mass is constant over the range of dissociation energies and oxide masses considered in this report.

3.3. Determining dissociation energy of unknowns

Using the correction term for mass from Fig. 3 and the bond energy calibration of Fig. 2, it is possible to estimate the dissociation energy of a diatomic oxide

Table 2

Dissociation energy determinations of unknowns using the empirical and theoretical correction terms for mass effects

| Element oxide ion | Literature D_0 (kJ mol ⁻¹) | Measured D_0 (kJ mol ⁻¹) |
|-------------------|--|--|
| YO ⁺ | 725 (±18) ^a | 718 (±25) |
| LaO ⁺ | 849 (±22) ^b | 875 (±25) |
| GdO ⁺ | 735 (±22) ^b | 724 (±25) |
| HoO ⁺ | 597 (±22) ^b | 551 (±25) |

^a See [20,21].

^b See [19] and references therein.

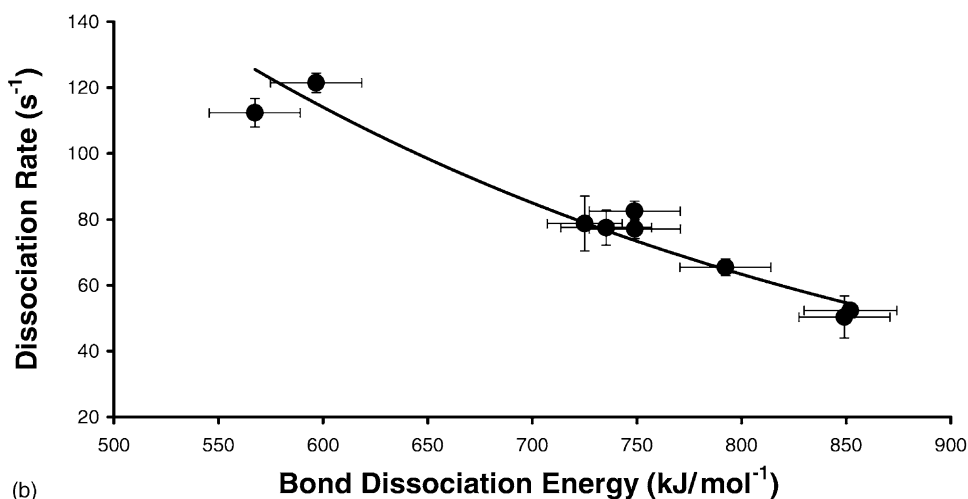
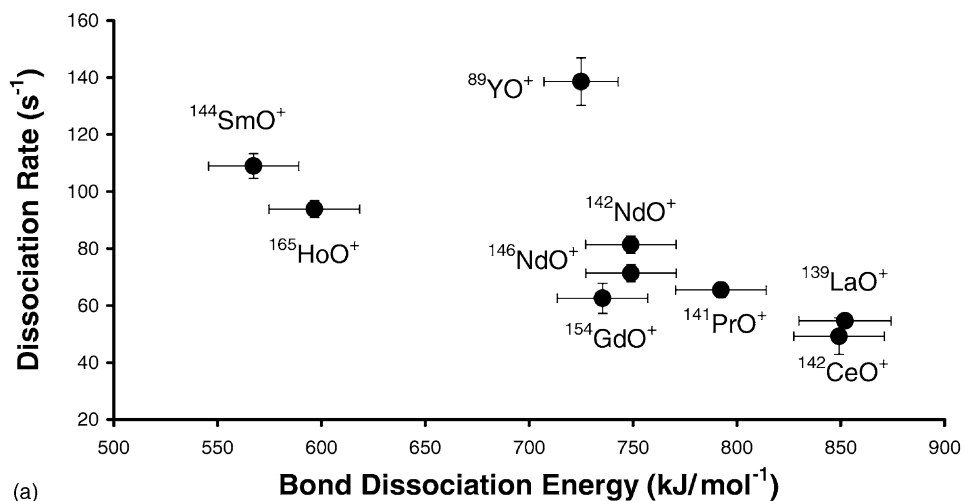


Fig. 4. Plot of dissociation rates as a function of bond dissociation (a) before and (b) after correction for mass effects.

ion from its dissociation rate and mass. Each of the oxide ions listed in Table 2 was dissociated under the conditions described above. These oxides were not included in the calibration curves and represent a range of bond energies and oxide ion masses. The dissociation rate was calculated from the corresponding fractional dissociation values following normalization to the value for praseodymium using Eq. (3). Finally, the equations for the curves in Figs. 2 and 3 were used to convert the rates to dissociation energies. The calculated dissociation energies are presented in Table 2. There is good agreement between the experimental results and those found in the literature. It should be noted that this method provides an estimate of bond dissociation energy with an internal precision that is equivalent to the interlaboratory precision calculated from literature values.

3.4. Bond strength and mass effects

Further evidence of the validity of the mass correction over the mass range of the lanthanide (plus yttrium) oxides and the correlation of measured rates to bond dissociation energy can be seen when the corrected and uncorrected CID rates are compared for the suite of elements. The dissociation rates for all the lanthanide oxide ions in Tables 1 and 2 (normalized to that for PrO^+) are shown in Fig. 4a. This plot shows that without taking into account the influence of mass on the rate measurement, there is very little correlation between dissociation rate and bond strength ($R^2 = 0.51$). Some correlation exists because of the limited mass range of the lanthanide elements. Because the mass of each ion and its affect on dissociation rate is known, it is possible to adjust the measured rates using the empirical correction

$$nk_{\text{corr}} = nk_{\text{meas}}(1 + 1.15(M_{\text{LnO}^+} - M_{\text{PrO}^+})) \quad (4)$$

where nk_{corr} is the empirically corrected dissociation rate and nk_{meas} is the measured dissociation rate. Fig. 4b is a plot of the rates from Fig. 4a that have been adjusted using Eq. (4). It is clear that once the mass effects are removed there is a strong relationship between the dissociation rate and bond strength

($R^2 = 0.94$), making it possible to construct a calibration curve of different bond dissociation energies that can be used in the determination of such values for an unknown.

4. Conclusions

The method used in this project to make dissociation rate measurements is sensitive to the mass of the dissociating ion. The sensitivity of the rate on mass can be empirically corrected by producing a calibration curve of compounds having the same bond strength but different masses. The slope of this curve can be used to account for the influence of mass on CID rate. Mass-corrected CID rates can then be used to provide a relationship between bond strength and dissociation rate. Over the range of masses and voltages studied, it was also possible to obtain an estimate for D_0 values based on such corrections.

The dynamic range of the calibration curve is currently limited to the oxide ions that dissociate at similar excitation voltages as the internal standard, praseodymium oxide. Although we are able to dissociate high mass and strongly bound diatomic oxide ions (e.g., UO^+) with unit efficiency, the voltage required to effect a detectable dissociation rate falls beyond the resonance excitation voltage used for our calibration curve. Thus, the effect of voltage on dissociation rate measurements will be an important consideration in extending the working range of this method.

Ongoing investigations focus on refining the thermal reaction model for CID to take into account the effect of mass on dissociation rate with the goal of refining the predictive capabilities of the model in light of new empirical evidence. Future work will also consider other diatomic systems such as metal sulfides to test the applicability and universality of the mass and bond energy calibrations. Application of this technique to small polyatomic ions such as metal methoxides and hydroxides will extend our understanding and the utility of this approach to polyatomic systems. Understanding both mass and voltage effects will enable a rapid probe for the determination of

dissociation/fragmentation energetics—particularly important for organometallic and organic ions.

Acknowledgements

Research sponsored by the Division of Chemical Sciences, Geosciences, and Biosciences, Office of Basic Energy Sciences, U.S. Department of Energy, under contract DE-AC05-00OR22725 with Oak Ridge National Laboratory, managed and operated by UT-Battelle, LLC. Discussions with Scott A. McLuckey of Purdue University in the early stages of this work are gratefully acknowledged.

References

- [1] D.C. Duckworth, D.E. Goeringer, S.A. McLuckey, *J. Am. Soc. Mass Spectrom.* 11 (2000) 1072.
- [2] D.E. Goeringer, S.A. McLuckey, *J. Chem. Phys.* 104 (1996) 2214.
- [3] D.E. Goeringer, S.A. McLuckey, *Rapid Commun. Mass Spectrom.* 100 (1996) 328.
- [4] D.E. Goeringer, K.G. Asano, S.A. McLuckey, *Int. J. Mass Spectrom.* 182/183 (1999) 275.
- [5] D.E. Goeringer, D.C. Duckworth, S.A. McLuckey, *J. Phys. Chem. A* 105 (2001) 1882.
- [6] F.L. King, W.W. Harrison, *Int. J. Mass Spectrom. Ion Processes* 89 (1989) 171.
- [7] D.C. Duckworth, R.K. Marcus, *Appl. Spectrosc.* 44 (1990) 649.
- [8] Y. Mei, D.C. Duckworth, P.R. Cable, R.K. Marcus, *J. Am. Soc. Mass Spectrom.* 5 (1994) 845.
- [9] J.T. Rowan, R.S. Houk, *Appl. Spectrosc.* 43 (1989) 976.
- [10] K.J. Hart, S.A. McLuckey, *J. Am. Soc. Mass Spectrom.* 5 (1993) 250.
- [11] F. Vedel, M. Vedel, J.S. Brodbelt, in R.E. March, J.F.J. Todd (Eds.), *Practical Aspects of Ion Trap Mass Spectrometry*, CRC Press, New York, 1995, p. 343.
- [12] A. Colorado, J. Brodbelt, *J. Am. Soc. Mass Spectrom.* 7 (1996) 1116.
- [13] M.J. Charles, S.A. McLuckey, G.L. Glish, *J. Am. Soc. Mass Spectrom.* 5 (1994) 1031.
- [14] S.A. McLuckey, *J. Am. Soc. Mass Spectrom.* 3 (1991) 599.
- [15] G.C. Stafford, P.E. Kelly, J.E.P. Syka, W.E. Reynolds, J.F.J. Todd, *Int. J. Mass Spectrom. Ion Processes* 60 (1984) 85.
- [16] D.E. Goeringer, K.G. Asano, S.A. McLuckey, D. Hoekman, S.W. Stiller, *Anal. Chem.* 66 (1994) 313.
- [17] J.N. Louris, R.G. Cooks, J.E.P. Syka, P.E. Kelly, J.G.C. Stafford, J.F.J. Todd, *Anal. Chem.* 59 (1987) 1677.
- [18] G.P. Jackson, D.C. Duckworth, D.E. Goeringer, Unpublished results.
- [19] M.S. Chandrasekharaiah, K.A. Gingerich, in J.K.A. Gschneidner, L. Eyring (Eds.), *Handbook on the Physics and Chemistry of the Rare Earths*, Elsevier, New York, 1989, p. 409.
- [20] M.R. Seivers, Y. Chen, P.B. Armentrout, *J. Chem. Phys.* 105 (1996) 6322.
- [21] D.E. Clemmer, N.F. Dalleska, P.B. Armentrout, *Chem. Phys. Lett.* 190 (1992) 259.